

Fast Decoding Algorithm for Subspace and Subsystem Color Codes and Local Equivalence of Topological Phases

Guillaume Duclos-Cianci¹, Héctor Bombín², and David Poulin¹

¹*Département de Physique, Université de Sherbrooke, QC, Canada and*

²*Perimeter Institute for Theoretical Physics, Waterloo, ON, Canada*

(Dated: October 14, 2010)

Topological codes introduced by Kitaev [9] are among the most promising family of quantum error correcting codes that could lead to realistic quantum computer architectures. Many features of these codes explain why they can operate reliably in the presence of a considerable amount of noise, with a threshold of nearly 1% [10]. First, it is possible to implement many gates on the qubits encoded in these codes in a purely topological or transversal fashion. Both of these methods are important because they directly result in fault-tolerant gates. Second, the syndrome extraction involves measurements of only four neighboring qubits on a two-dimensional lattice. This is to be contrasted with, e.g., concatenated codes where the number of qubits involved in each syndrome measurement grows linearly with the size of the code, thus increasing the complexity of the error correction procedure and lowering the threshold.

The most general method to protect quantum information is not of a subspace code, but a subsystem code. Recently one of us introduced the family of topological subsystem color codes (TSCC) [2], which pushes the features of topological codes to their extreme. Indeed, the syndrome extraction for these codes requires only two-qubit measurements, as simple as it can possibly get. Additionally, the entire Clifford group can be performed in a topological fashion on the qubits encoded in these codes. For these reasons, TSCC may well be the simplest and most efficient means of achieving fault tolerance.

To be of any practical use, any error-correcting code must have an efficient decoder—an algorithm that finds the most likely recovery given the measured error syndrome. Recently, two of us have conceived a decoding algorithm for Kitaev’s toric code (KTC) that is exponentially faster than previously known decoding algorithms (run time $\log \ell$ rather than ℓ^6 where ℓ is the linear size of the torus) [7]. Note that the decoding run-time is a crucial factor for fault tolerance; proofs of the threshold theorem usually assume instantaneous classical side-computation to assist the error-correction procedure. Our algorithm is also very flexible, it enables various tradeoffs between complexity and error-correction performances. In particular, we were able to demonstrate that it can achieve a higher error-correction error threshold than what was achievable by previously known decoding algorithms [6, 8].

Here, we demonstrate how this fast decoding algorithm, as well as other decoding algorithms, can be ap-

plied to a wider class of topological error correcting codes. We do this by demonstrating a local equivalence between various codes. More precisely, we consider the family of topological color codes (TCC) [4] and their subsystem cousins TSCC [2, 3] and show that they can be locally mapped to a number of copies of KTC. That is, local in the sense that an operator with support on qubits contained within a region of finite radius r is mapped to an operator with support within a region of radius $c + r$, where c is some constant.

As a consequence of this local equivalence, we can, for the purpose of decoding, treat a topological code as a certain number of copies of KTC, and use any decoding algorithm suitable for KTC to complete the decoding on each of these copies. Crucially, the noise model induced on KTC remains essentially local: an error model that is independent on each qubit will be mapped to an error model with some short range correlations on a length scale c , but no long range correlation. Because the existence of an error threshold is essentially a large scale property of a system, this decoding strategy should also produce a finite error threshold, albeit with a different critical error probability that depends on the value of c and other microscopic details of the mapping.

The importance of this decoding strategy for the TSCC can be stressed by the fact that, to our knowledge, it provides the first example of a family of subsystem codes with an efficient decoding algorithm. The general construction of Bacon and Casaccino [1] for instance can produce subsystem codes with sparse gauge operators, a close analogue of classical LDPC codes, but unfortunately have no known decoding algorithm. Another motivation comes from Bravyi’s recent proof that geometrically local subsystem codes are much more powerful than geometrically local subspaces codes in that they can achieve better tradeoffs between minimal distances and encoding rates [5].

Our fast decoding algorithm makes use of methods of statistical physics and classical coding theory, namely renormalization group methods and belief propagation [11]. Details of this decoding algorithm can be found in [7]. Here, we will focus on the local mapping between topological codes. To understand the intuition behind these mappings, it is useful to think of a subspace error correcting code as a local Hamiltonian

$$H = - \sum_a S_a, \quad \text{with } [S_a, S_b] = 0 \quad (1)$$

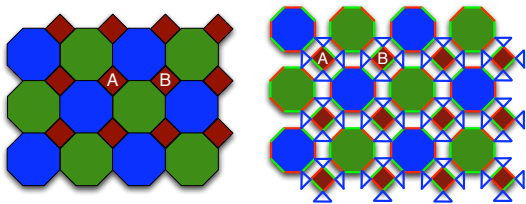


Figure 1. (left) Regular 4-8 tiling for TCC. The diamonds can be labeled A or B according to a chessboard pattern, depending on the color green or blue of the octagon located on its upper left. (right) Expanded 4-8 tiling for TSCC. Starting with the 4-8 lattice, each vertex is expanded into a triangle.

where the S_a are stabilizers generators defining the code space $\mathcal{C} = \{|\psi\rangle : S_a|\psi\rangle = |\psi\rangle, \forall a\}$. In this language, the code space is the degenerate ground space of the Hamiltonian, and errors can cause excitations in the system—a local energy increase above the ground energy. The excitations are anyons that carry a charge, that can be defined by a notion of local equivalence. Consider a finite region of the system that contains some errors, in such a way that not all stabilizer generators supported on that region take value +1. Two such excitation patterns carry the same topological charge if it is possible to change one's error syndrome into the other's syndrome by a unitary transformation acting only on that region. In other words, errors E and E' have the same charge on region \mathcal{R} if there exists a unitary transformation U acting trivially outside \mathcal{R} such that $[S_a, E] = [S_a, UE'U^\dagger]$ for all S_a supported on region \mathcal{R} .

With this definition, we can say that KTC has four topological charges, the vacuum (0) corresponding to no excitations, an electric charge (e) corresponding to a plaquette excitation, a magnetic charge (m) corresponding to a star excitation, and a composite excitation (f) containing both. Any error on a finite region can be mapped to one of these three possibilities. Excitations with different charges are also characterized by different braiding statistics, that describe the effect of exchanging two excitations of the same charge. For KTC, both the electric and magnetic particles are bosons because they have trivial braiding statistics, while the composite particle is a fermion because it acquires a -1 sign upon particle exchange. Excitations with different charges can also have non-trivial mutual braiding statistics, that describes the effect of wrapping one excitation around the other. In KTC, all mutual statistics are semionic. Finally, two charges can merge to form a new charge, and these are dictated by the fusion rules $m \times e \rightarrow f$ and $\sigma \times \sigma \rightarrow 0$ for $\sigma = m, e, f$. The notion of topological charge is important because local mappings preserve the charge content of a model.

The first example we consider is the TCC defined on a 4-8 regular tiling of Fig. 1. Qubits are located at the vertices of this tiling, and there are two stabilizer operators

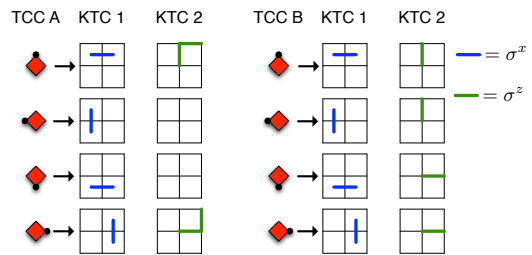


Figure 2. Mapping between the Pauli operators of the 4-8 TCC and two copies of Kitaev's code KTC1 and KTC2. The black dots indicate the location of a Pauli σ^x operator on the TCC. Each of these operators gets mapped to a Pauli operator that can have support on the two copies of KTC. The qubits on the KTC are located on the edges of the lattice. As indicated by the legend, a blue (green) line indicates a σ^x (σ^z) operator on the corresponding qubit. The mapping depends on the location on the chessboard coloring, so there is one mapping defined for A diamonds and one for B diamonds. not shown here is a similar mapping for the σ^z operators of the TCC.

associated to every plaquette p

$$S_p^\sigma = \bigotimes_{j \in \partial p} \sigma_j, \quad \text{with } \sigma \in \{\sigma^x, \sigma^z\} \quad (2)$$

where ∂p is the set of vertices of the plaquette p and σ^x, σ^z are the usual Pauli matrices. The excitations in this model can carry 16 different topological charges, 10 bosons and 6 fermions. These, as well as all the mutual statistics, correspond exactly to the charges obtained from two copies of KTC. A detailed consideration of the statistics and mutual statistics of the two models leads to a mapping shown at Fig. 2. It was obtained by identifying elementary excitations with the same topological charges and mutual statistics in the two codes. It can easily be verified that this mapping also transforms the local stabilizer generators of one code into local stabilizer generators of the other codes. Thus, the syndrome information is readily available for decoding the KTCs after the stabilizers of the TCC have been measured. Figure 3 shows the performances of the resulting decoding algorithm on a bit-flip channel.

The second example we consider is the TSCC of the 4-8 expanded lattice of Fig. 1. Qubits are located on the vertices of the lattice, and there is one gauge group generator associated to each edge e

$$G_e = \bigotimes_{j \in \partial e} \sigma_j \quad (3)$$

with $\sigma = \sigma^x, \sigma^y$, or σ^z for a red, green, or blue edge respectively, and ∂e denotes the set of vertices adjacent to the edge. The stabilizers are the center of the gauge group, and they also admit a local set of generators (of weight 24). This code has four topological charges that are all fermions (f_1, f_2, f_3) except the vacuum and all

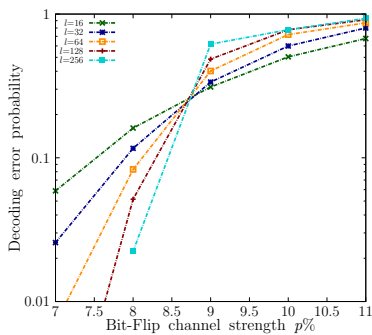


Figure 3. Decoding error probability as a function of the bit-flip probability for the 4-8 TCC decoded using a local mapping to two KTC decoded and the algorithm of [7]. The different curves illustrate lattices of different size: below a threshold probability of roughly 8.7%, the decoding error probability decreases with the lattice size, leading to a perfect recovery in the thermodynamic limit. The optimal threshold for this code is around 11%.

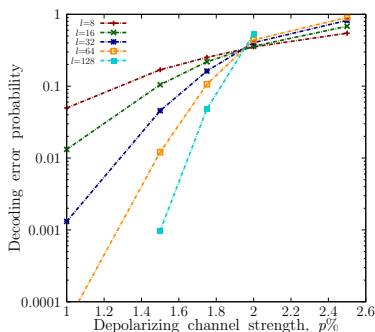


Figure 4. Same as Fig. 3 for the 4-8 topological subsystem color code. The threshold we obtain is about 2%.

have fermionic mutual statistics. The fusion rules are $f \times f \rightarrow 0$ and $f_i \times f_j \rightarrow f_k$ when i, j, k are all different. These can be obtained from a subset of the topological charges of two copies of KTC. One can identify for instance $f_1 \leftrightarrow (f, 0)$, $f_2 \leftrightarrow (e, f)$, and $f_3 \leftrightarrow (m, f)$. With this mapping in hand, we were able to decode the TSCC by reducing the problem to that of decoding two copies of KTC. Our simulation results are shown at Fig. 4, with a threshold of roughly 2%.

Conclusion—We have demonstrated that distinct topological codes can be mapped onto each other by local

transformations. This enables to use any decoding algorithm suitable for one of these codes to decode any other code that is locally equivalent. We have illustrated this idea with the topological color code and the topological subsystem color code, that had no previously known efficient decoding algorithm. These local mappings could have additional use for fault-tolerant quantum computation. In particular, one could in principle take advantage of all the codes that are locally equivalent by switching between them during the computation in a fault tolerant fashion.

Acknowledgements—This work was supported in part by MITACS, NSERC, and FQRNT. Computational resources were provided by the Réseau québécois de calcul de haute performance (RQCHP) and Compute Canada.

-
- [1] D. BACON AND A. CASACCINO, *Quantum error correcting subsystem codes from two classical linear codes*, arXiv:quant-ph/0610088v2, (2006).
 - [2] H. BOMBIN, *Topological subsystem codes*, Physical Review A, 81 (2009), p. 32301.
 - [3] H. BOMBIN, *Clifford gates by code deformation*, arXiv:1006.5260v1 [quant-ph], (2010).
 - [4] H. BOMBIN AND M. A. MARTIN-DELGADO, *Topological quantum distillation*, Physical Review Letters, 97 (2006), p. 180501.
 - [5] S. BRAVYI, *Subsystem codes with spatially local generators*, Arxiv preprint arXiv:1008.1029, (2010).
 - [6] E. DENNIS, A. KITAEV, A. LANDAHL, AND J. PRESKILL, *Topological quantum memory*, Journal of Mathematical Physics, 43 (2002), p. 4452.
 - [7] G. DUCLOS-CIANCI AND D. POULIN, *Fast decoders for topological quantum codes*, Physical Review Letters, 104 (2009), p. 050504.
 - [8] J. W. HARRINGTON, *QECC : symplectic lattice and toric codes*, California Insitute of Technology, (2004).
 - [9] A. Y. KITAEV, *Fault-tolerant quantum computation by anyons*, ANNALS PHYS., 303 (2003), p. 2.
 - [10] R. RAUSSENDORF, J. HARRINGTON, AND K. GOYAL, *Topological fault-tolerance in cluster state quantum computation*, New Journal of Physics, 9 (2007), p. 199.
 - [11] J. S. YEDIDIA, W. T. FREEMAN, AND Y. WEISS, *Constructing free energy approximations and generalized belief propagation algorithms*, IEEE Transactions on Information Theory, 51 (2005), pp. 2282–2312.